IEEE Access
Multidisciplinary | Rapid Review | Open Access Journal

Received May 23, 2019, accepted June 22, 2019, date of publication July 8, 2019, date of current version July 25, 2019.

Digital Object Identifier 10.1109/ACCESS.2019.2927217

Comparative Analysis of Channel Models for Industrial IoT Wireless Communication

WENBO WANG[1], (Student Member, IEEE), STEFAN L. CAPITANEANU[2], (Member, IEEE), DANA MARINCA[3], (Member, IEEE), AND ELENA-SIMONA LOHAN[1], (Senior Member, IEEE)

[1]Electrical Engineering Unit, Tampere University, 33210 Tampere, Finland
[2]Schneider Electric, 75002 Rueil-Malmaison, France
[3]PRISM Unit, University Paris Saclay, 78035 Saint-Aubin, France

Corresponding author: Wenbo Wang (wenbo.wang@tuni.fi)

This work was supported by the Academy of Finland under Project PRISMA, project number 313039.

ABSTRACT In the industrial environments of the future, robots, sensors, and other industrial devices will have to communicate autonomously and in a robust and efficient manner with each other, relying on a large extent on wireless communication links, which will expand and supplement the existing wired/Ethernet connections. The wireless communication links suffer from various channel impairments, such as attenuations due to path losses, random fluctuations due to shadowing and fading effects over the channel and the non line-of-sight (NLoS) due to obstacles on the communication path. Several channel models exist to model the industrial environments in indoor, urban, or rural areas, but a comprehensive comparison of their characteristics is still missing from the current literature. Moreover, several IoT technologies are already on the market, many competing with each other for future possible services and applications in Industrial IoT (IIoT) environments. This paper aims at giving a survey of existing wireless channel models applicable to the IIoT context and to compare them for the first time in terms of worst-case, median-case, and best-case predictive behaviors. Performance metrics, such as cell radius, spectral efficiency, and outage probability, are investigated with a focus on three long-range IoT technologies, one medium-range, and one short-range IoT technology as selected case studies. A summary of popular IoT technologies and their applicability to industrial scenarios is addressed as well.

INDEX TERMS 3GPP channel loss models, cell radius, industrial IoT, outage probability, spectral efficiency.

I. INTRODUCTION AND MOTIVATION

Sensors and devices inter-connected through various Internet of Things (IoT) protocols can improve the production steering and ensure a more efficient end-to-end traceability and surveillance along the production chain, provided that the IoT wireless communication links are properly designed to support the target spectral efficiency with minimal interruption levels and limited bandwidth. The IoT wireless communication links span over a wide area of carrier frequencies, from existing centimeter-wave (cmWave) links to future millimetre-wave (mmWave) connections and support a wide area of bandwidths, from Ultra Narrow Band (UNB) communications (such as Sigfox, Telensa, and Weightless-N standards) to spread spectrum (e.g., LoRa, ZigBee, WirelessHART, Ingenu, WAVIoT) and even wideband communications (e.g., WiFi-based IoTs) [1].

The IoT devices can also be classified according to their power consumption. A classification of IoT technologies which can be used in industrial applications is shown in Fig. 1. The IoT solutions can be grouped into low-power (LP) or battery-operated solutions, and high-power (HP) solutions. Each of these two categories can be further grouped according to the communication ranges, into short (e.g., few meters to few tens of meters), medium (e.g., few tens of meters to few kilometers), and long ranges (e.g., ranges up to few tens of km). The vast majority of IoT standards nowadays fall under the LP category (several IoT standards names are enumerated in Fig. 1; details on each standard can be found for example in [1]). The high-power/high-throughput

The associate editor coordinating the review of this manuscript and approving it for publication was Qing Yang.

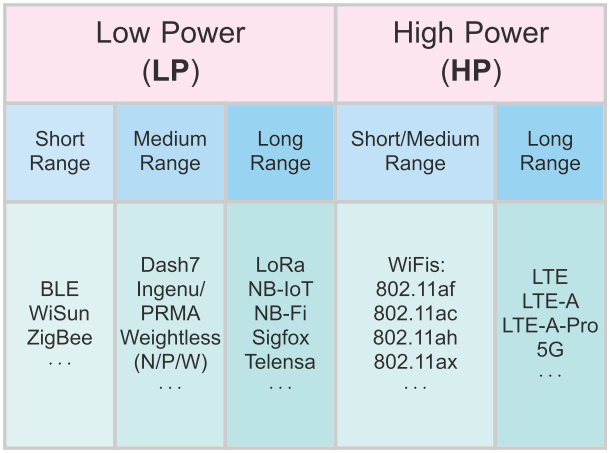

FIGURE 1. Classifications of the connectivity solutions for industrial applications.

solutions are covered by current and emerging Wireless Local Area Networks (WLAN) standards, popularly known as WiFis, and by the cellular communications, such as the existing 4G/Long Term Evolution (LTE) standards and the emerging 5G standard [2], [3].

Industrial IoT market will form a significant part of the future Information, Communication and Technology (ICT) markets [4]. Communications links in IIoT will have to trade the high spectral efficiency for low battery consumption and long-range support [5]. Thus, there will be no winning IIoT technology for all possible applications. Wireless IIoT solutions are meant to enable a predictive management of wireless equipment used at various industrial sites, to increase the workers' safety and production capacity [6], to increase the savings of stakeholders involved in the industrial chain [7], to enable wireless self-localization of electronic devices and components in 3D industrial space [8], etc.

Examples of potential industrial applications for existing IoT technology are summarized in Table 1 for 18 of the most encountered IoT solutions. The communication range is specified for each of these technologies, together with existing uses in IIoT. A 'not available' (n/a) input does not mean that such technology cannot be used in that particular scenario, but rather that, to the best of the authors' knowledge, no industrial solutions have been tested so far under that particular scenario. The considered scenarios are divided into: rural, urban, and indoor, according to the typical classification of channel models [9], but it is worth mentioning that the boundaries between these three scenarios are not very strict.

No prevalent IoT technology for industrial applications exist, as the choice of a good technology should rely on a multi-criterion decision making process [10], [11], which takes into account the ease of installation and maintenance of a certain technology, its scalability and robustness, its privacy, its power consumption, and its range.

Three widely encountered long-range IoT technologies in industrial applications are LoRa (e.g., flower industry [12], chemical emission monitoring [13], etc.), Sigfox, and NB-IoT. One novel medium-range industrial IoT technology is MIOTY, claiming that it is the first technology following the European Telecommunications Standards Institute (ETSI) low throughput networks standard [14]. One widely encountered short-range technology in industrial IoT is ZigBee. These five technologies, namely NB-IoT, LoRa, Sigfox, MIOTY, and ZigBee, are selected as case studies in our paper, but we remark that similar studies for additional IoT technologies are straightforward to implement based on the methodology presented here.

In order to accurately model the wireless communication links between any two IoT devices, one acting as a transmitter and the other one as a receiver, a link budget analysis is always necessary and it needs to rely on a specific channel model. Link budget refers to balancing the received powers in uplink and downlink directions, by taking into accounts the transmission powers, the antenna gains, and the losses encountered over the wireless propagation channel. The channel modeling typically includes the distance-dependent and deterministic path losses, and the spatio-temporal random effects due to shadowing, multipath, and Doppler effect.

To the best of the authors' knowledge, no comprehensive analysis of existing channel models and their applicability to industrial IoT environments exist and this is the gap we plan to address in our paper. The authors' main contributions are: (1) the analysis of the benefits of the path-loss channel modeling for IIoT applications, (2) the comprehensive description of path-loss channel models for various IIoT technologies (as the formulas presented in here cannot be found in an unified form elsewhere, to the best of the authors' knowledge), (3) the derivation of best-case, median-case, and worst-case bounds for rural, urban, and indoor scenarios for IIoT applications based on existing path-loss models, and (4) the analysis of five IIoT case studies, relying on five different IoT technologies, in terms of cell radius, spectral efficiency, and outage probabilities.

The rest of the paper is organized as follows. In Section II, we briefly discuss the importance of channel modeling in designing an IIoT system. An comprehensive description and discussion of channel loss models are given in Section III. Section IV lists the link budget and other information of selected IoT technologies, NB-IoT, LoRa, Sigfox, Zigbee and MIOTY. In Section V, VI and VII, three metrics, namely the coverage area, spectral efficiency and outage probability, are studied based the selected IoT technologies in Section IV. Section VIII concludes this work and provides some insights of open research in IIoT.

II. THE BENEFITS OF ADEQUATE PATH-LOSS CHANNEL MODELING FOR THE IIOT APPLICATIONS

As already mentioned in the first section, the wireless channel modeling part plays an essential role in choosing the right IIoT technology and building efficient IIoT solutions. An adequate channel modeling allows a designer to estimate and forecast the losses and random fluctuations over the signal power when sent information over a wireless link.

TABLE 1. Visions of industrial applications per IoT technology type according to the channel scenario.

	Technology	Range	Rural (forest industry, agriculture, etc.)	Urban	Indoor (warehouses, mines, industrial halls, etc.)
Low power	BLE/BLE mesh	short	n/a	Smart metering	Smart warehouses with fully automated 3D storage system
	Dash 7	medium	Food monitoring and tracking		
	EC GSM-IOT	long	Monitoring temperature fluctuations in the cold chain or other supply chains; predictive maintenance of goods in a supply chain		n/a
	Ingenu/RPMA	long	Utility monitoring and management (street lightening, hot-water heaters, cool pumps, etc.)		n/a
	LoRa	long	Remote control of industrial sensors in harsh environments (indoor air quality monitoring, liquid presence detectors, industrial temperature monitoring, etc.); smart asset management; waste management		
	NB-Fi (WAVIoT)	long	Remote temperature control in stored food; smart metering; environmental sensing for worker safety (CO2 level, moisture level, etc.)		
	NB-IoT	long	Utility management, asset tracking	Security control	Factory lightening
	Sigfox	long	Tracking workers for safety/geofencing alerts		
	Telensa	long	Utility monitoring		
	Weightless N/P/W	medium	n/a	Smart metering	Shelf autonomous updating
	WeightlessHART	short	n/a	Industrial process control and asset management	
	WiSUN	short	n/a	Smart utility network	
	ZigBee/ZigBee-NaN	short	n/a	Industrial control and sensing applications	
	MIOTY	medium	Mining, gas and oil	Smart metering and industrial sensing applications	
	Wirepass Mesh	long	n/a	Smart metering, factory lighting and asset tracking	
High power	WiFi	long	n/a	Remote control and monitoring of industrial equipment, electronic instrumentation	
	LTE/LTE-A/LTE-A-Pro	long	Industrial gateways in harsh environments	Remote control and monitoring	
	5G	long	Smart manufacturing, smart utility networks, remote energy control, augmented and virtual reality-based industrial solutions, etc.		

The designer could also use the channel models to approximate the cell radius or coverage areas for a particular technology, the outage probabilities under a certain network topology or Access Node (AN) density, the required dimensions of the infrastructure (e.g. number and placement of ANs), etc. Being able to model accurately the wireless channel effects is an important step towards a reliable and efficient design of a wireless IIoT solution. With the help of the channel models, a designer is able to:

- Estimate the operational Signal-to-Noise Ratio (SNR) for a particular industrial application in a particular environment;
- Estimate the density of access nodes required to cover a certain industrial area;
- Estimate the uplink (UL) and downlink (DL) coverage areas and balance the link budgets (i.e., the received powers in UL and DL directions);
- Understand if a certain IoT technology is suitable only in a specific scenario (e.g., rural versus urban) or can be easily scaled to various scenarios;
- Estimate the spectral efficiency of a certain network in terms of supported number of sensors or nodes and achievable throughput under limited bandwidth;
- Allow an efficient network planning in IIoT and reduce the installation and maintenance costs;
- Enable a predictive management of equipment, e.g., predicting failures in various electronic components and ensure their timely replacement;

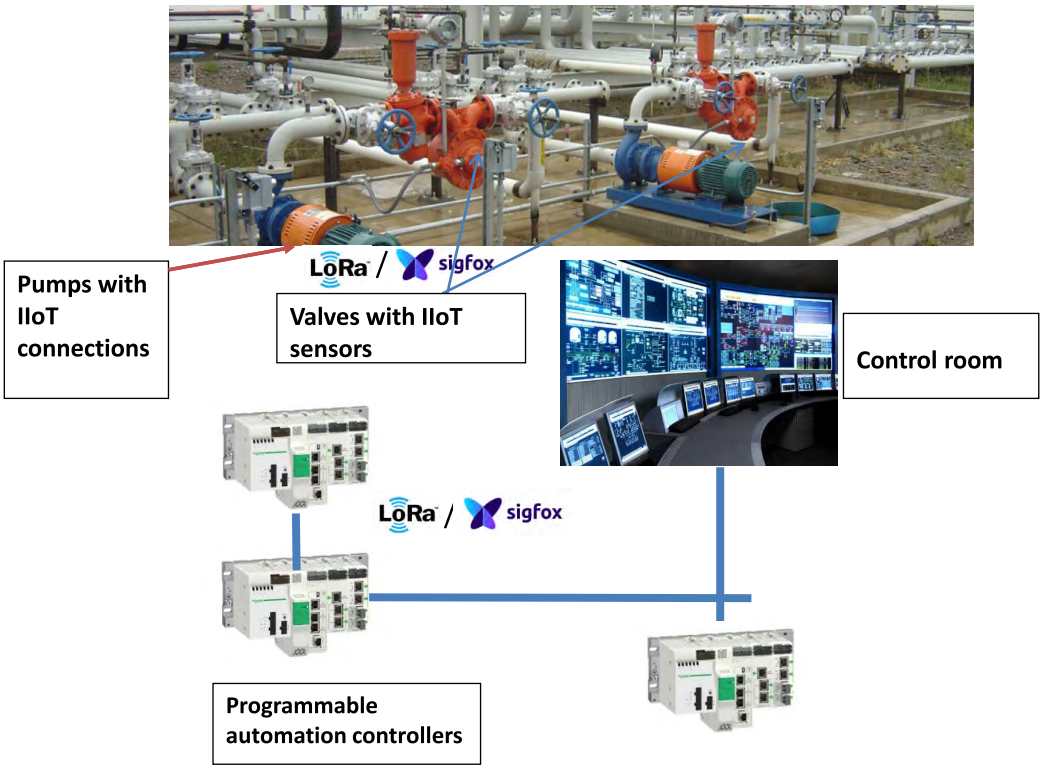

FIGURE 2. Example of an outdoor IIoT application: Pumps with IoT sensors.

- Permit cost savings through remote control and updating of various components and devices in the industrial chain (e.g., yard and asset management, fleet tracking, etc.);
- Facilitate the wireless geo-localization of captor industrial sensors and other measurement sensors.

Different IIoT applications may operate in different scenarios, such as rural versus urban, or outdoor versus indoor. Thus, it makes sense that the channel models to be used will also be adapted to the scenario targeted by a particular application.

An example of outdoor IIoT application, for both urban and rural cases, is illustrated in Fig. 2: the distribution pumps (e.g., for water, gas, or petrol) can be equipped with IoT sensors, e.g., based on a long-range IoT technology such as LoRa or Sigfox, and the sensors can transmit in a timely manner anomalies in the distribution chain to a control center, as well as they can enable an optimization of the distribution and they can control the pressure and flow in the pipes.

Another IIoT example, this time for an indoor scenario, is illustrated in Fig. 3 for a building management system based on ZigBee (or other short-range IoT) sensors. The IoT sensors would permit to remotely monitor the installation at every level, from the incoming circuit breaker to the final electrical load. The IoT sensors would also ensure real-time alarms and email notifications for voltage loss and overload trips, pre-alarm notifications in the event of an overload, etc.

The channel modeling for IIoT applications has yet to be addressed in detail in the existing literature. From the state-of-the-art in this field it is worth mentioning that a channel model for industrial applications based on LoRa technology has previously been studied in [12]. It was shown in [12] that up to 6000 nodes can be served with a single access node (or gateway) in an indoor industrial area with a surface of 34000 m^2, assuming a simplified single-slope path-loss channel model with measurement-fit coefficients, as described in [15]. No comparison between various channel models was given in [12]. Another path-loss model based on LoRa was studied in [16] for indoor IIoT applications. The channel model in there relied on a two-slope simplified path-loss model and was not validated by measurements. Other channel models proposed in the literature for IIoT applications are variants of the simplified single-path model, e.g., a single-slope path loss model for ZigBee indoor IIoT applications [17], a single-slope path loss model for generic Received Signal Strength (RSS) estimation, with parameters adjustable according to the temperatures [18].

In addition to the literature dedicated to IoT applications, 3GPP has been developing more general channel models, covering various 5G applications scenarios, from terrestrial to aerial communications and from LP to HP applications and they have been grouping them under three main categories: rural, urban, and indoor [9]. The 3GPP models will be discussed in Section III. The applicability of the 3GPP indoor

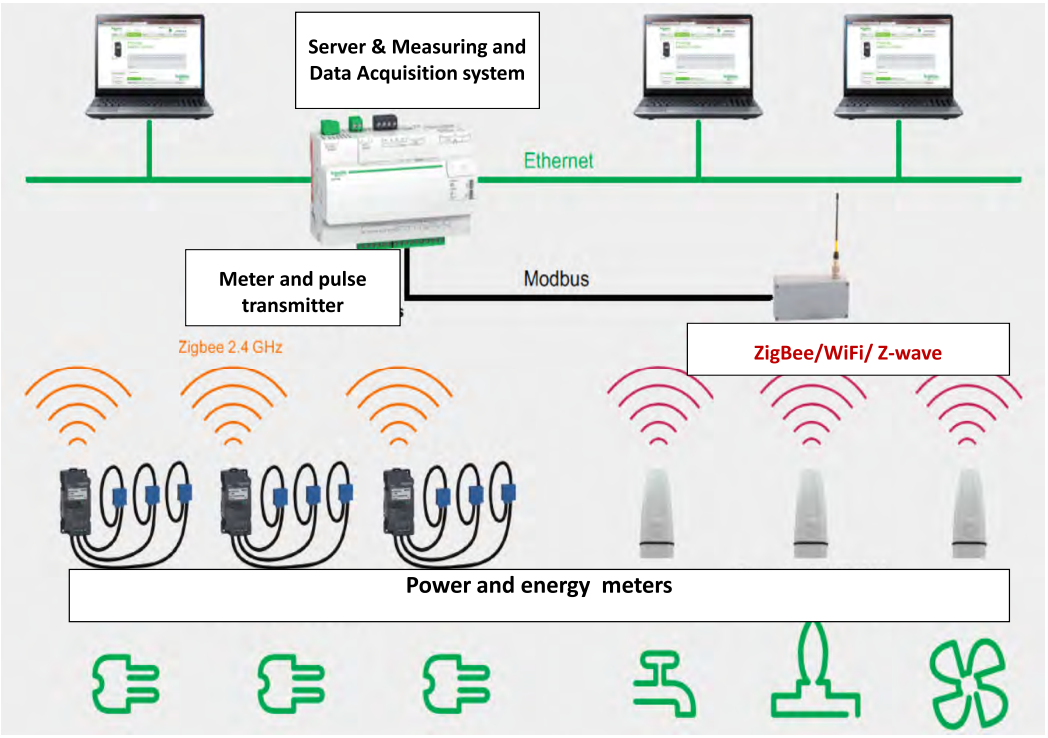

FIGURE 3. Example of an indoor IIoT application: Building management system with energy and power metering.

hotspot channel model to IIoT scenarios has been also studied previously by the authors in [19]. However, only the indoor propagation models were analyzed in [19] and the conclusion was that outage probabilities constraints in industrial IoT can be reached with cmWave propagation, but more research is needed to improve the achievable spectral efficiency and outage probabilities in mmWave ranges under the considered indoor scenarios.

As seen above, there is only a limited coverage of the path-loss channel modeling applicable to IIoT scenarios in the existing literature and a comparison between the existing models under both outdoor and indoor scenarios is still lacking. In addition, most of the reported models rely on a single-slope path loss model with environment-dependent parameters (i.e., apparent transmit power and path-loss coefficient) and they require scenario-specific measurement campaigns to estimate the model parameters. In what follows we describe several path-loss models developed in the existing literature for rural, urban, and indoor scenarios and we will look at the worst-case, median-case, and best-case predicted values under different metrics in order to be able to pinpoint the most relevant models in the context of IIoT.

III. ANALYSED CHANNEL MODELS

A variety of wireless terrestrial channel models has been developed in the literature and a designer has typically a wide pool to choose from. However, in the context of IIoT, a comparison between the main features of these different channel models is hard to find in the existing literature. The next sub-sections present seven identified wireless channel models from the literature and discuss their applicability in an IIoT context: the free space loss model, the single-slope model, the 3GPP models (four variants, according to target scenario, detailed in Table 4 and 6), and the industrial indoor channel models (two variants, detailed in Table 4). Additionally, the industrial environment is complex, and usually featured by large obstacles, multiple reflections and frequent movements. To tackle with these issues, the shadowing is used to model the effect caused by the large obstructions in the propagation path and the small-scale fading is used to model the effect caused by the multipath and the movement of subjects in the environment. The discussion of shadowing and small-scale fading follows the descriptions of the channel loss models in each sub-section. In Sections V, VI and VII, we will analyze and compare numerically the channel models with fixed parameters (i.e., by dropping out the single-slope channel model, which is a generic model, with an infinity of possible parameters), in terms of various metrics relevant to industrial environments.

A. FREE SPACE LOSS MODEL

The **Free Space Loss (FSL)** model is often used as a theoretical lower bound and a performance benchmark in all wireless channel modeling studies. Its advantages stay in its low complexity, its low number of parameters, and its easy mathematical tractability. Its main drawback is the fact that it is usually too idealistic to measure practical industrial environments and can offer only a very loose bound

in performance, as it will be also obvious from our studies in Sections V, VI and VII. FSL has been used as a bound also in other IoT-related studies, for example for wireless propagation over sandy terrains [20] or in oil rigs [21].

In a FSL, the received power P_R (in dB) at a distance d_{3D} (in m) from the transmitter is given by,

$$P_R = P_T - PL_{FSL}(d_{3D}) \quad (1)$$

where P_T is the transmit power and PL_{FSL} is the free space path loss in dB scale defined in Table 4.

The shadowing and small-scale fading is not applicable in FSL model.

B. SINGLE-SLOPE SIMPLIFIED PATH LOSS MODEL

The generic single-slope path loss model is encountered in a vast majority of papers [17], [18], [22] related to wireless communications. This model is given in terms of received signal strength P_R according to two parameters: an apparent transmit power and a path-loss (or slope) coefficient:

$$P_R = P_{T_a} - 10n\log_{10}(d_{3D}) \quad (2)$$

where n is the path loss coefficient, P_{T_a} is the apparent transmit power, typically measured as the power at 1 m away from the transmitter. The carrier frequency effect is implicitly included in the P_{T_a}, but it does not appear any more as a model parameter.

In this simplified (and generic) model, the path loss coefficient n and P_{T_a} are typically derived based on measurements and are valid only for a particular scenario. The shadowing and small-scale fading are usually modeled as additive random variables following the log-normal distribution and Rician distribution respectively. The simplicity of the model makes it widely adopted by many research papers [17], [18], but the fact that n and P_{T_a} do not have unique values makes it unsuitable to be included in a comparison as such. Indeed, FSL can be seen as particular case of this simplified single-scope model.

C. 3GPP OUTDOOR AND INDOOR CHANNEL MODELS

3GPP standardization has been recently dedicated a significant amount of work for modeling the terrestrial wireless channels for a variety of applications, in particular related to the New Radio (NR) and 5G developments. The 3GPP channel models are built on a multitude of parameters determined empirically from various measurement campaigns and they have been grouped into three main categories: rural, urban, and indoor. In [9], terrestrial channel models that could be widely applied from 0.5 GHz to 100 GHz carrier frequency were proposed. In [3] the extension of models up to 300 m (300 m altitude is usually considered as the low altitude) is presented.

All 3GPP channel loss models describe the shadowing effects as additive random variables following zero-mean log-normal distribution $\mathcal{N}(0, \sigma^2)$ (details see Appendix A Table 4). The small-scale fading is modeled as additive random variables following Rician distribution Rice(K) (details see Appendix A Table 5).

1) 3GPP RMA

The **Rural Macrocell (RMa)** model of 3GPP [9] characterizes the channel loss of rural areas with a base station height h_{BS} (in meter), a robot height h_{UT} (in meter), an average street width W (in meter), and an average building height h (in meter). In 3GPP RMa model, the height of base station is assumed to range from 10 m to 50 m, the height of robot is from 1 m to 10 m, the street width is from 5 m to 50 m, the building height is from 5 m to 50 m. The model uses a breakpoint distance d_{BP} (in meter) concept to divide the path loss calculation into two parts: i) one with the horizontal distance d_{2D} (in meter) smaller than breakpoint distance and ii) the other with the horizontal distance greater than breakpoint distance.

In Appendix A Table 4, eq. (12) and (13) are path loss in RMa line-of-sight (LoS) and non-line-of-sight (NLoS) scenarios, respectively. Table 6, eq. (22) gives the LoS probability for 3GPP RMa scenario.

2) 3GPP UMA

The **Urban Macrocell (UMa)** model of 3GPP [9] characterizes the channel losses of urban areas in the situation when the base station antenna is above rooftops. 3GPP UMa model is constructed also taking into account the base station height and robot height. The height of base station ranges from 10 m to 50 m, the height of robot ranges from 1.5 m to 22.5 m. Similarly with the 3GPP RMa model, 3GPP UMa model also uses the breakpoint distance concept d'_{BP} (in meter) to divide the path loss calculation into two parts. However, unlike the 3GPP RMa model, it approximates the breakpoint distance by taking into account the effective environment height h_E (in meter) rather than only considering base station height and robot height as in 3GPP RMa model.

In Appendix A Table 4, eq. (14) and (15) show the path loss in UMa LoS and NLoS scenarios, respectively. Table 6, eq. (23) gives the LoS probability in UMa scenario. The effective environment height yields to eq. (3a), the effective antenna height of robot h'_{UT} (in meter) and the effective antenna height of base station h'_{BS} (in meter) are given in eq. (3b) and (3c),

$$h_E = \begin{cases} h_{UT} \le 13 \text{ m} \quad \text{or} \quad d_{2D} \le 18 \text{ m}, \\ 1; \\ 13 \text{ m} < h_{UT} \le 22.5 \text{ m} \quad \text{and} \quad d_{2D} > 18 \text{ m}, \\ \frac{5}{4}\left(\frac{h_{UT}-13}{10}\right)^{1.5}\left(\frac{d_{2D}}{100}\right)^3 e^{\left(-\frac{d_{2D}}{150}\right)}. \end{cases} \quad (3a)$$

$$h'_{UT} = h_{UT} - h_E \quad (3b)$$

$$h'_{BS} = h_{BS} - h_E \quad (3c)$$

3) 3GPP UMI

The **Urban Microcell (UMi)** model of 3GPP [9] characterizes channel loss of urban areas in the situation when the base station antenna is below rooftops. 3GPP UMi model also takes into account the base station height and robot height. The height of base station is set to 10 m in the 3GPP UMi and the height of robot is from 1.5 m to 22.5 m. Like 3GPP RMa and UMa models, 3GPP UMi model uses a breakpoint distance d'_{BP} concept as well and applies the exact breakpoint distance calculation as the UMa model. However, in UMi model the effective environment height is defined as 1 m.

In Appendix A Table 4, eq. (16) and (17) are path loss in UMi LoS and NLoS scenarios, respectively, in Table 6, eq. (24) gives LoS probability in UMi scenario.

4) 3GPP INH

The Indoor Hotspot (InH) model of 3GPP [9] characterizes channel loss in indoor areas where low mobility of objects, strong reflection of signals and many obstacle of path are existed. InH model is categorized into two cases: i) **the mixed office (InHm)** and ii) **the open office (InHo)**. The difference in the two categories stays in the LoS probability calculation, which allows higher probability of LoS situation in open office than in mixed office. In Appendix A Table 4, eq. (18) and (19) are path loss in InH LoS and NLoS scenarios respectively, in Table 6, eq. (25) gives LoS probability in mixed office case, eq. (26) gives LoS probability in open office case.

D. INDUSTRIAL INDOOR CHANNEL LOSS MODEL

In [23], an industrial indoor channel loss model is proposed according to an extensive measurement campaign. The channel loss model focuses on the Industrial Scientific Medical (ISM) band, namely 900 MHz, 2400 MHz and 5200 MHz. In the paper, our interest is the channel characteristics in 900 MHz and 2400 MHz, whose path loss models are given in Appendix A Table 4, eq. (20) and eq. (21).

The model gives considerations of two scenarios: the low multi-path effect scene and the high multi-path effect scene. Moreover, the movements of obstacles in the environment and the movements of receivers/transmitters are also taken into account.

The shadowing effect is characterized as additive random variables following zero-mean log-normal distribution $\mathcal{N}(0, \sigma^2)$ (details see Appendix A Table 4). The small-scale fading is modeled as additive random variables following Rician distribution Rice(K) (details see Appendix A Table 5).

E. OVERALL PATH-LOSS MODEL USED IN OUR STUDIES

In some channel models (e.g., 3GPP models in section III-C), channel loss is investigated in LoS and NLoS situations, while others (e.g., the industrial indoor model in section III-D), channel loss is given without distinguishing LoS and NLoS situations. In order to use the channel loss models reviewed in this section to evaluate different IoT technologies in Section V, VI and VII, here we define an overall path loss model as follows,

$$PL_{\mathrm{overall}} = \mathrm{Pr}_{\mathrm{LOS}}(L_{\mathrm{LOS}}) + (1 - \mathrm{Pr}_{\mathrm{LOS}})(L_{\mathrm{NLOS}}) + \zeta \quad (4)$$

where PL_{overall} denotes the overall path loss, $\mathrm{Pr}_{\mathrm{LOS}}$ denotes the LoS probability, ζ denotes the small-scale loss, L is defined as the total large-scale loss,

$$L_{\mathrm{LOS/NLOS}} = PL_{\mathrm{LOS/NLOS}} + \xi_{\mathrm{LOS/NLOS}} \quad (5)$$

where $PL_{\mathrm{LOS/NLOS}}$ denotes the path loss median value in the LoS or NLoS situation, $\xi_{\mathrm{LOS/NLOS}}$ denotes the shadowing loss in the LoS or NLoS situation.

TABLE 2. Link budgets for various IoT solutions (Downlink).

Parameters	NB-IoT (standalone)	LoRa (*SF=12)	Sigfox	Zigbee	MIOTY [27]
Modulation	**OFDM	**CSS	**UNB	**DSSS	**TS-UNB
Transmit power [dBm]	43	14	27	20	14
Bandwidth (B) [kHz]	180	125	0.6	2000	25
Receiver Noise Figure [dB]	5	5	5	5	8
Maximum Coupling loss (MCL) [dB]	164	151	161	118	154
Receiver Sensitivity [dBm]	-121	-137	-134	-98	-140
Carrier Frequency [MHz]	900	868	868	2400	868

*SF denotes spreading factor. In LoRa technology, the receiver sensitivity is −137 dBm when the SF is 12;
**OFDM denotes Orthogonal Frequency Division Multiplexing, CSS denotes Chirp Spread Spectrum, UNB denotes Ultra Narrow-Band, DSSS denotes Direct Sequence Spread Spectrum, TS-UNB denotes Telegram-Splitting-Ultra-Narrow-Band [14].

IV. LINK BUDGETS USED IN OUR ANALYSES

The link budget of a system reflects many aspects in the transmitter-receiver chain, for example, the maximum coupling loss, the trade-off between bandwidth and transmitted power. As motivated in the introductory sections, we select five technologies, namely NB-IoT, LoRa, Sigfox, Zigbee and MIOTY, to present and compare their link budget. Based on [14], [24]–[27], the link budget is shown in Table 2.

Among NB-IoT, LoRa, Sigfox, Zigbee and MIOTY technologies, NB-IoT promises the best tolerance of coupling loss (i.e., 164 dB) in the transmitter-receiver chain, Zigbee has the highest bandwidth (i.e., 2 MHz), and MIOTY with TS-UNB modulation provides the best receiver sensitivity (i.e., −140 dBm).

V. COVERAGE AREAS

In this section, we applied both the reviewed channel loss models from Section III and the link budgets from Section IV

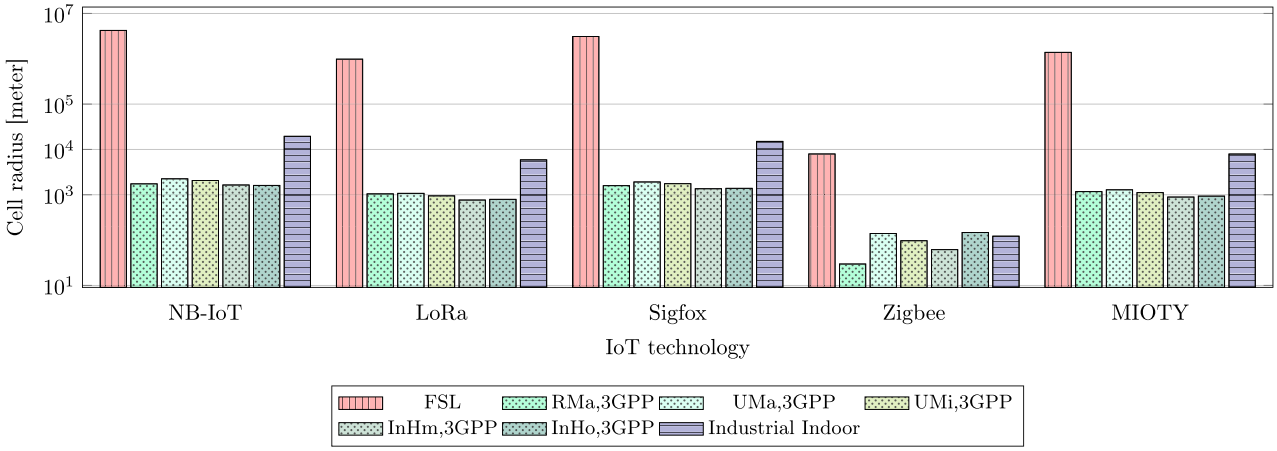

FIGURE 4. Cell radius of different technologies under different channel loss models at 1% outage probability. (FSL denotes Free Space Loss; RMa,3GPP denotes 3GPP Rural Macrocell; UMa, 3GPP denotes 3GPP Urban Macrocell; UMi, 3GPP denotes 3GPP Urban Microcell; InHm, 3GPP denotes 3GPP Indoor hotspot mixed office; InHo, 3GPP denotes 3GPP Indoor Hotspot open office; Industrial Indoor denotes Industrial Indoor channel loss model.).

to estimate the radius of a cell coverage area according to a target outage probability at cell edges. With a specific target metric, for example the target bit rate or the target outage probability, we could find the boundary of a cell service coverage area.

The outage probability is defined as the probability that overall path loss in (4) is greater or equal to maximum coupling loss. This is the minimum requirement that maintains connection of a wireless link. The mathematical expression is,

$$P_{\text{out}} = \Pr(PL_{\text{overall}} \geq \text{MCL}) \tag{6}$$

We set the outage probability P_{out} equal to 1% and find the appropriate horizontal distance (i.e., the cell radius). In this estimation, we assumed that the height of robot is 2 m, the height of access node (AN) is 10 m, the average height of buildings is 5 m and the average width of street is 20 m. The cell radius predicted by different channel models at 1% outage probability are shown in Fig. 4. The best-case is clearly predicted by FSL, but it is overly optimistic. The worst-case and median-case are also numerically shown in Table 3, and compared with other values reported in the literature.

In Table 3 we also presented the reported or measured cell range for comparison purposes. For example, in Sigfox technology, reported range from [31] is from 3000–10000 m, however in [32] the authors measured 600 m cell range in urban area. Our median-case predictors, obtained with 3GPP channel modeling, seem to predict quite close the average reported values for these technologies from other researchers. From Fig. 4 and Table 3, based on the models we reviewed, NB-IoT clearly beats the other four technologies with a median cell range 2061 m. Sigfox also has a good coverage with a median cell range 1754 m. Zigbee has the worst coverage, as expected, since it is targeting for short-range IoT applications.

Last but not the least, we would like to highlight that from the point of view of the cell radius study, the 3GPP models seem the most reasonable models to approximate the channel path losses. From Fig. 4, the FSL usually gives an upper bound of cell radius; the industrial indoor model fails to predict the cell radius when the MCL is large, due to the unbelievable large predicted cell radius. The NB-IoT, LoRa, Sigfox and MIOTY are assumed to be candidates in the industrial indoor applications, however according to the cell radius estimated by the industrial indoor model, the above four technologies have better coverage in indoor rather than in outdoor (e.g., the results from 3GPP UMa), which is unlikely to be true. The industrial indoor model, nevertheless, provides some insight in the Zigbee technology, according to its prediction of cell radius, the industrial indoor environment is in between indoor open office and mixed office.

TABLE 3. Cell range of different technologies.

Technology	Predicted cell range from studied models		Cell range measured or reported from literatures
	worst value [m]	median value [m]	reported value [m]
NB-IoT	1609	2061	1000–8000 in [28]
LoRa	765	1046	3400 in [29], 2000 in [30]
Sigfox	1356	1754	3000–10000 in [31], 600 in [32]
Zigbee	29.7	122	30–50 in [33]
MIOTY	890	1712	claimed 5 km urban/ 15 km flat terrains [27]

VI. SPECTRAL EFFICIENCY

In most of the IoT technologies which can be applied to various industrial sites, the achievable spectral efficiency may

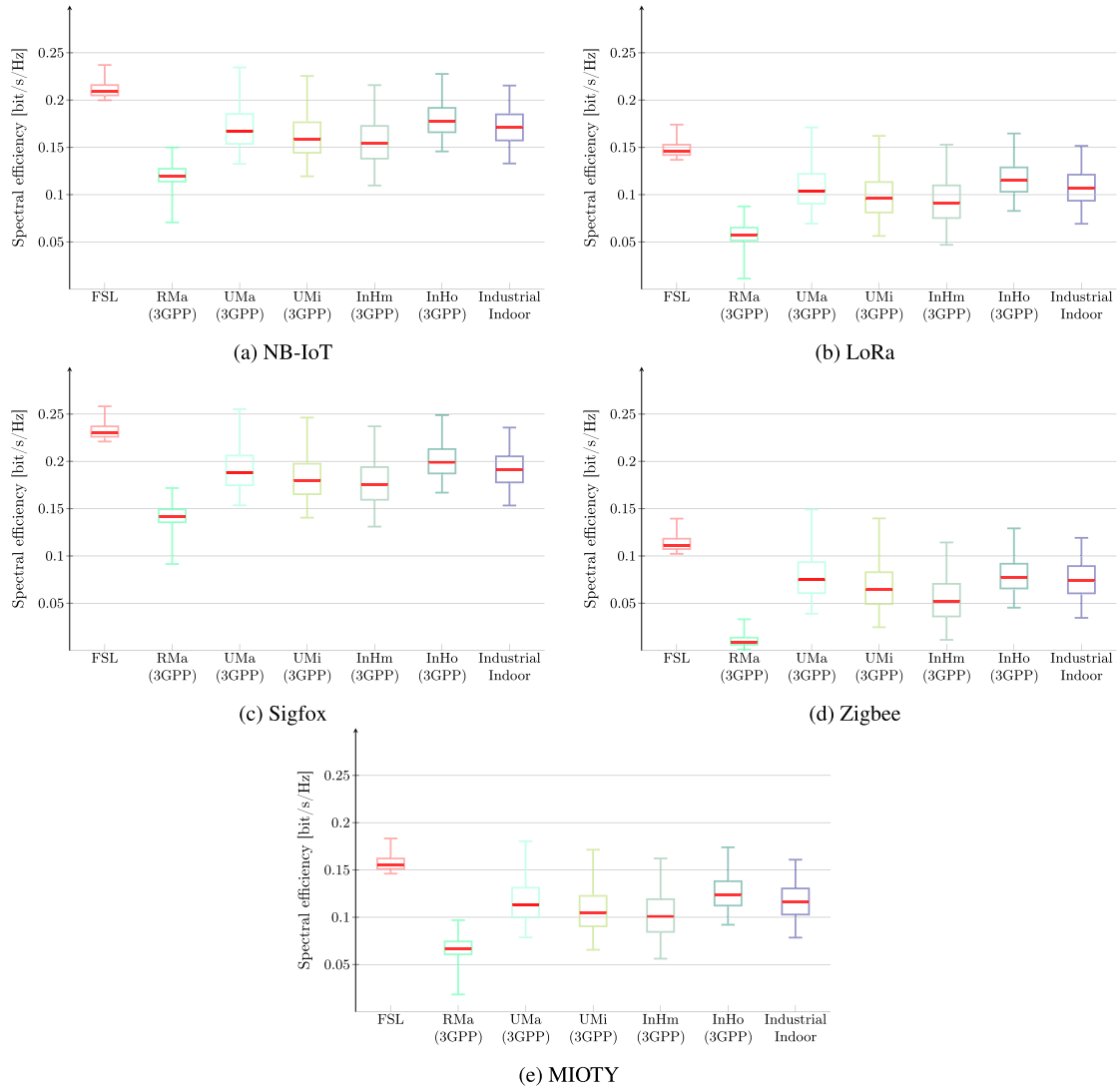

FIGURE 5. Spectral efficiency comparisons among NB-IoT, LoRa, Sigfox, Zigbee and MIOTY technologies. The result is based on 100 Monte Carlo runs (the Monte Carlo method is a statistical sampling technique [34], [35]).

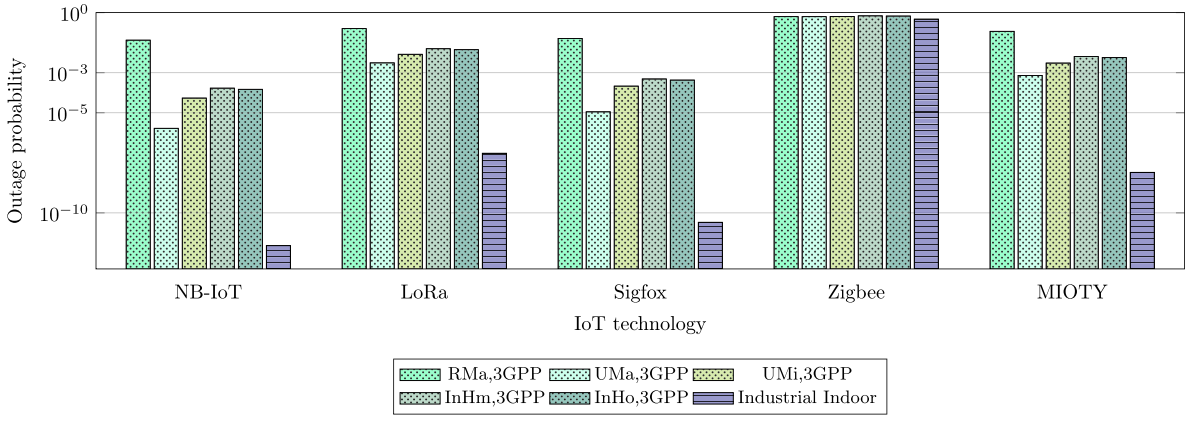

FIGURE 6. Outage probability of different technologies under different channel loss models.

vary in a large extent due to different industrial environments. This section analyses the five selected IoT technologies in terms of spectral efficiency.

The spectral efficiency C (in bits per second per Hz or bit/s/Hz) is limited by the duty cycle of certain devices [36], in the downlink, the spectral efficiency is

TABLE 4. Channel loss models with shadowing.

		Path loss in decibel, d_{3D} in meter, f_c in GHz	Parameters
FSL	n/a	$PL_{\text{FSL}} = 32.45 + 20\log_{10}(d_{3D}) + 20\log_{10}(f_c)$ (11)	n/a
3GPP RMa [9]	LOS	$\begin{cases} 10\,\text{m} \le d_{2D} \le d_{\text{BP}}, \quad \sigma_{\text{LOS1}} = 4 \\ PL_{\text{LOS1}} = 20\log_{10}\left(\frac{40\pi d_{3D} f_c}{3}\right) + \min(0.03h^{1.72}, 10)\log_{10}(d_{3D}) \\ \qquad - \min(0.044h^{1.72}, 14.77) + 0.002\log_{10}(h) d_{3D} \\ d_{\text{BP}} < d_{2D} \le 10\,\text{km}, \quad \sigma_{\text{LOS2}} = 6 \\ PL_{\text{LOS2}} = PL_{\text{LOS1}}(d_{\text{BP}}) + 40\log_{10}\left(\frac{d_{3D}}{d_{\text{BP}}}\right) \end{cases}$ (12)	$d_{\text{BP}} = 2\pi h_{\text{BS}} h_{\text{UT}} f_c / C$, $C = 3 \times 10^8$ m/s, $10\,\text{m} \le h_{\text{BS}} \le 150\,\text{m}$, $1\,\text{m} \le h_{\text{UT}} \le 10\,\text{m}$, $5\,\text{m} \le W \le 50\,\text{m}$, $5\,\text{m} \le h \le 50\,\text{m}$, f_c is carrier frequency in Hz, d_{2D} is horizontal distance, d_{3D} is 3D distance C is speed of light, d_{BP} or d'_{BP} is breakpoint distance in meter, h_{BS} is height of base station, h_{UT} is height of robot, W is average street width, h is average building height, σ is standard deviation of Gaussian variables, which are used to model shadowing effect.
	NLOS	$PL_{\text{NLOS}} = \max(PL_{\text{LOS}}, PL'_{\text{NLOS}}), \quad \sigma_{\text{NLOS}} = 8$ $\begin{aligned} PL'_{\text{NLOS}} = {} & 161.04 - 7.1\log_{10}(W) + 7.5\log_{10}(h) - \left(24.37 - 3.7(h/h_{\text{BS}})^2\right)\log_{10}(h_{\text{BS}}) \\ & + \left(43.42 - 3.1\log_{10}(h_{\text{BS}})\right)\left(\log_{10}(d_{3D}) - 3\right) \\ & + 20\log_{10}(f_c) - \left(3.2\left(\log_{10}(11.75h_{\text{UT}})\right)^2 - 4.97\right) \end{aligned}$ (13)	
3GPP UMa [9]	LOS	$\begin{cases} 10\,\text{m} \le d_{2D} \le d'_{\text{BP}}, \quad \sigma_{\text{LOS1}} = 4 \\ PL_{\text{LOS1}} = 28.0 + 22\log_{10}(d_{3D}) + 20\log_{10}(f_c) \\ d'_{\text{BP}} < d_{2D} \le 5\,\text{km}, \quad \sigma_{\text{LOS2}} = 4 \\ PL_{\text{LOS2}} = 28.0 + 40\log_{10}(d_{3D}) + 20\log_{10}(f_c) - 9\log_{10}\left((d'_{\text{BP}})^2 + (h_{\text{BS}} - h_{\text{UT}})^2\right) \end{cases}$ (14)	$d'_{\text{BP}} = 2\pi h'_{\text{BS}} h'_{\text{UT}} f_c / C$, h'_{BS} and h'_{UT} are effective antenna height, $h'_{\text{BS}} = h_{\text{BS}} - h_{\text{E}}$, $h'_{\text{UT}} = h_{\text{UT}} - h_{\text{E}}$, h_{E} is effective environment height, $1.5\,\text{m} \le h_{\text{UT}} \le 22.5\,\text{m}$, $h_{\text{BS}} = 25\,\text{m}$, *in d_{BP} or d'_{BP}, the f_c is in Hz, in other places, f_c is in GHz.
	NLOS	$PL_{\text{NLOS}} = \max(PL_{\text{LOS}}, PL'_{\text{NLOS}}), \quad \sigma_{\text{NLOS}} = 6$ $PL'_{\text{NLOS}} = 13.54 + 39.08\log_{10}(d_{3D}) + 20\log_{10}(f_c) - 0.6(h_{\text{UT}} - 1.5)$ (15)	
3GPP UMi [9]	LOS	$\begin{cases} 10\,\text{m} \le d_{2D} \le d'_{\text{BP}}, \quad \sigma_{\text{LOS1}} = 4 \\ PL_{\text{LOS1}} = 32.4 + 21\log_{10}(d_{3D}) + 20\log_{10}(f_c) \\ d'_{\text{BP}} < d_{2D} \le 5\,\text{km}, \quad \sigma_{\text{LOS2}} = 4 \\ PL_{\text{LOS2}} = 32.4 + 40\log_{10}(d_{3D}) + 20\log_{10}(f_c) - 9.5\log_{10}\left((d'_{\text{BP}})^2 + (h_{\text{BS}} - h_{\text{UT}})^2\right) \end{cases}$ (16)	$h_{\text{E}} = 1\,\text{m}$, $1.5\,\text{m} \le h_{\text{UT}} \le 22.5\,\text{m}$, $h_{\text{BS}} = 10\,\text{m}$.
	NLOS	$PL_{\text{NLOS}} = \max(PL_{\text{LOS}}, PL'_{\text{NLOS}}), \quad \sigma_{\text{NLOS}} = 7.82$ $PL'_{\text{NLOS}} = 22.4 + 35.3\log_{10}(d_{3D}) + 21.3\log_{10}(f_c) - 0.3(h_{\text{UT}} - 1.5)$ (17)	
3GPP InH [9]	LOS	$PL_{\text{LOS}} = 32.4 + 17.3\log_{10}(d_{3D}) + 20\log_{10}(f_c), \quad \sigma_{\text{LOS}} = 3$ (18)	$1\,\text{m} \le d_{3D} \le 150\,\text{m}$.
	NLOS	$PL_{\text{NLOS}} = \max(PL_{\text{LOS}}, PL'_{\text{NLOS}}), \quad \sigma_{\text{NLOS}} = 8.03$ $PL'_{\text{NLOS}} = 17.3 + 38.3\log_{10}(d_{3D}) + 24.9\log_{10}(f_c)$ (19)	
Industrial indoor [23]	900 MHz	$PL = 61.65 + 24.9\log_{10}(d_{3D}/15), \quad \sigma = 7.35$ (20)	n/a
	2400 MHz	$PL = 71.84 + 21.6\log_{10}(d_{3D}/15), \quad \sigma = 8.13$ (21)	

given by,

$$C = \eta D_{\text{d}} \log_2(1 + \text{SNR}) \tag{7}$$

where SNR denotes signal-to-noise-ratio in linear scale, D_{d} denotes duty cycle, η denotes channel efficiency, in this section η was taken equal to 0.7. The duty cycle D_{d} is

regulated in [37] in Europe, 1% duty cycle is maximum that can be used in 868 MHz ISM band. Here, we remark that the NB-IoT uses legacy band, no duty cycle restriction has been put on to it. However, in order to compare spectral efficiency metrics of all selected IoT technologies in Section IV, we use 1% duty cycle for NB-IoT as well.

Fig. 5 compares achievable spectral efficiency under different channel path-loss models and under five different IoT technologies. The high spectral efficiency is more relevant at short ranges (i.e., indoor applications), than at large ranges, thus our example here focuses on a 200 × 200 m^2 square indoor industrial site. Here we consider 5% outliers, which the ends of the whiskers are represented by the 2.5th percentile and the 97.5th percentile respectively.

The height of robot remains 2 m, the height of AN remains 10 m as in section V. We note that in this scenario, 3GPP UMi, InHm, InHo and industrial indoor channel loss models are more relevant to the indoor applications than the others, thus the results discussion will focus more on these four models. In NB-IoT technology, InHo model predicts the highest median value 0.178 bit/s/Hz; InHm model with almost 0.154 bit/s/Hz median value gives the lower bound of NB-IoT spectral efficiency. In LoRa, Sigfox, Zigbee and MIOTY technologies, a similar situation occurs to them as well, in the sense that InHo model predicts the highest median value of spectral efficiency while InHm model gives the lowest median value. Among these five technologies, the Sigfox is most spectral efficient technology in the indoor scenarios, the Zigbee is the worst technology from the spectral efficiency aspect. However, the Zigbee at 2.4 GHz frequency band has 2 MHz bandwidth resource and it could provide the highest throughput among these five technologies in indoor scenarios.

VII. OUTAGE PROBABILITY

IIoT technologies could also serve many kinds of outdoor applications, as discussed in Section I. In a large outdoor area, the outage probability metric (i.e., one dimension of reliability) usually has priority over spectral efficiency. Therefore, in this section, we define a 2000 × 2000 m^2 simulation area to compare different IIoT services. The height of robot and base station are still 2 m and 10 m, respectively. From Table 1, we remark that Zigbee is a short range IoT technology, thus the main discuss of this section focuses on NB-IoT, LoRa, Sigfox and MIOTY only. Besides, we will pay more attentions to the outdoor channel loss models, for example, the 3GPP RMa, UMa and UMi models.

In this section, we calculate the average outage probability over the entire simulation space. Let the set $\mathcal{S}$ denote all positions of a robot in simulation space, a position of a robot is $\mathbf{s}_i \in \mathcal{S}$, in Cartesian coordinate system $\mathbf{s}_i$ is defined as,

$$\mathbf{s}_i = \{x_i, y_i, z_i : x_i, y_i \in (-10^3, 10^3), z_i \in (0, 2)\} \quad (8)$$

TABLE 5. K-factor for small-scale fading.

Model	K-factor [dB]
3GPP RMa [9]	$K \sim \mathcal{N}(7, 4^2)$
3GPP UMa [9]	$K \sim \mathcal{N}(9, 3.5^2)$
3GPP UMi [9]	$K \sim \mathcal{N}(9, 5^2)$
3GPP InH [9]	$K \sim \mathcal{N}(7, 4^2)$
Industrial Indoor [23]	900 MHz $K = 11.5$ 2400 MHz $K = 11.6$

where $i = 1, 2, 3, \cdots$, the average outage probability $\overline{P}_{\text{out}}$ is defined as,

$$\overline{P}_{\text{out}} = \frac{\sum_{\mathbf{s}_i \in \mathcal{S}} P_{\text{out}}^{(\mathbf{s}_i)}}{|\mathcal{S}|} \quad (9)$$

where $P_{\text{out}}^{(\mathbf{s}_i)}$ denotes eq. (6) at $\mathbf{s}_i$.

Under the considerations of shadowing and small-scale fading effects, the analytic solutions of $P_{\text{out}}^{(\mathbf{s}_i)}$ are hard to find. The shadowing effects are usually modeled as random variables (in dB) following Gaussian distribution, while the small-scale fading effects are modeled as random variables (in linear scale) following Rician distribution. In this paper, we estimate $P_{\text{out}}^{(\mathbf{s}_i)}$ by treating its solution as the tail probability estimation in *sum of non-identically distributed random variables situation* [35]. The algorithm 10.6 in [35] is applied, the $P_{\text{out}}^{(\mathbf{s}_i)}$ is estimated by,

$$P_{\text{out}}^{(\mathbf{s}_i)} = \Pr(\mathcal{X}^{(\mathbf{s}_i)} \geq \text{MCL} - PL^{(\mathbf{s}_i)}) \quad (10)$$

where $PL^{(\mathbf{s}_i)}$ is the deterministic part of the path loss, $\mathcal{X}^{(\mathbf{s}_i)}$ denotes the sum of shadowing and small-scale fading effects at $\mathbf{s}_i$, MCL $- PL^{(\mathbf{s}_i)}$ is the threshold in the algorithm 10.6 in [35].

As seen in Fig. 6, NB-IoT outperforms LoRa, Sigfox and MIOTY IoT technologies in terms of outages. The worst case for NB-IoT is predicted by the 3GPP RMa model with 3.76×10^{-2} outage probability. Generally speaking, NB-IoT, LoRa, Sigfox and MIOTY has their most outages events in the RMa scenarios from the results. Among 3GPP RMa, UMa and UMi models, the predictions of UMa model are always the best cases, for example, 1.42×10^{-6} outage probability in NB-IoT, 2.67×10^{-3} outage probability in LoRa, 9.40×10^{-6} outage probability in Sigfox, 6.46×10^{-4} outage probability in MIOTY.

VIII. CONCLUSIONS AND OPEN RESEARCH DIRECTIONS

In this work, we addressed the problem of wireless channel modeling in the context of IIoT technologies. We described

TABLE 6. Line-of-sight probability for 3GPP models.

Model	Line-of-sight probability
3GPP RMa [9]	$\Pr = \begin{cases} 1, & d_{2D} \le 10\,\text{m} \\ e^{-\frac{d_{2D}-10}{1000}}, & 10\,\text{m} < d_{2D} \end{cases}$ (22)
3GPP UMa [9]	$\Pr = \begin{cases} 1, & d_{2D} \le 18\,\text{m} \\ \left(\frac{18}{d_{2D}} + \left(1-\frac{18}{d_{2D}}\right)e^{-\frac{d_{2D}}{63}}\right)\left(1+\frac{5}{4}C'(h_{UT})\left(\frac{d_{2D}}{100}\right)^3 e^{-\frac{d_{2D}}{150}}\right), & 18\,\text{m} < d_{2D} \end{cases}$ (23) where $C'(h_{UT}) = \begin{cases} 0, & h_{UT} \le 13\,\text{m} \\ \left(\frac{h_{UT}-13}{10}\right)^{1.5}, & 13\,\text{m} < h_{UT} \le 23\,\text{m} \end{cases}$
3GPP UMi [9]	$\Pr = \begin{cases} 1, & d_{2D} \le 18\,\text{m} \\ \frac{18}{d_{2D}} + \left(1-\frac{18}{d_{2D}}\right)e^{-\frac{d_{2D}}{36}}, & 18\,\text{m} < d_{2D} \end{cases}$ (24)
3GPP InH [9]	Mixed office: $\Pr = \begin{cases} 1, & d_{2D} \le 1.2\,\text{m} \\ e^{-\frac{d_{2D}-1.2}{4.7}}, & 1.2\,\text{m} \le d_{2D} < 6.5\,\text{m} \\ 0.32e^{-\frac{d_{2D}-6.5}{32.6}}, & 6.5\,\text{m} \le d_{2D} \end{cases}$ (25) Open office: $\Pr = \begin{cases} 1, & d_{2D} \le 5\,\text{m} \\ e^{-\frac{d_{2D}-5}{70.8}}, & 5\,\text{m} \le d_{2D} < 49\,\text{m} \\ 0.54e^{-\frac{d_{2D}-49}{211.7}}, & 49\,\text{m} \le d_{2D} \end{cases}$ (26)

in details seven channel models, namely the free space loss, the 3GPP channel models with its five variants (indoor open and mixed hotspots, outdoor urban micro- and micro-cell, and outdoor rural), and the industrial indoor channel loss model for ISM bands. We also described the generic single-slope model, which is a generalization of FSL. We compared the predicted performance based on the above-mentioned seven channel models in terms of three important wireless communications metrics, namely the cell radius, the spectral efficiency, and the outage probability in both indoor and outdoor scenarios. We selected four potential IIoT technologies, namely NB-IoT, Sigfox, LoRA, ZigBee and MIOTY, to evaluate their performance in terms of cell radius at 1% outage probability, their spectral efficiency within $200\times200\,\text{m}^2$ area, and their outage probabilities within $2000\times2000\,\text{m}^2$ area.

Among these five potential IIoT technologies, NB-IoT has the longest cell radius and the best outage probability in outdoor scenarios, while Sigfox has the best spectral efficiency in indoor scenarios and Zigbee has the largest operating bandwidth. We have also shown that the median-case predictors among these studied channel models are not far from the values reported or measured in practice for the selected IIoT technologies. We would like to emphasize that 3GPP channel loss models are so far the best suitable models to estimate the studied communication metrics, as they often offer an estimate close to the median-predicted behavior by many other channel models. Considering the average of a certain metric over a space (i.e., the average spectral efficiency or outage probability over the simulation space), the worst-case scenario can be studied based on 3GPP RMa channel models, while the best-case scenario is given by the free-space loss channel model (i.e., overly optimistic bound).

In terms of future research work in IIoT environments, in our opinion, three key axes are: i) the wireless connection reliability, ii) the wireless geo-localization, and iii) the predictive maintenance. In our paper, the wireless connection reliability is thoroughly studied based on the channel loss models. The geo-localization and the predictive maintenance aspects will be investigated in the future work.

Regarding the reliability factor, extremely reliable wireless communication will be more and more needed in order to avoid heavy cabling in zones with difficult access.

For example, if we have a high furnace chimney where a quality air measurement device is to be installed, a wireless IoT sensor mounted on the top of the chimney may be 100 times less expensive than deploying an Ethernet cable from the top to the bottom of the tower. But a one hour stop of the IoT communication link may be 100 million times more expensive than the installation cost: NOx, SOx, or CO emission overrun during one hour may produce the closure of the plant.

Regarding the geo-localization needs, it is well-known that high expenses are engaged every time when a new person has to be trained for process operating in a plant. These expenses are increased by the turnover due to tedious working conditions. The wireless geo-localization of the devices from a specific installation may save lot of time and money and the autonomy of the new hired person would be dramatically improved.

Last, but not least, the predictive maintenance for large surface scattered installations may be easily deployed using precise reliable IIoT communication. The uploaded analytics from the field may predict dangerous increase or overrun of key indicators using low rate communicating systems at very low cost, much simpler to install than cabling.

APPENDIX A
CHANNEL LOSS MODELS AND LINE-OF-SIGHT PROBABILITY

See Table 4–6.

REFERENCES

[1] P. F. E. Silva, V. Kaseva, and E. S. Lohan, "Wireless positioning in IoT: A look at current and future trends," *Sensors*, vol. 18, no. 8, p. 2470, 2018.

[2] A. Gupta and E. R. K. Jha, "A survey of 5G network: Architecture and emerging technologies," *IEEE Access*, vol. 3, pp. 1206–1232, Jul. 2015.

[3] *Study on Enhanced LTE Support for Aerial Vehicles (Release 15)*, document 3GPP TR 36.777 v15.0.0, 3GPP-Technical Specification Group Radio Access Network, 2017. Accessed: Mar. 2018. [Online]. Available: http://www.3gpp.org/DynaReport/36-series.htm

[4] D. Miller, "Blockchain and the Internet of Things in the industrial sector," *IT Prof.*, vol. 20, no. 3, pp. 15–18, 2018.

[5] Y.-W. Kuo, C.-L. Li, J.-H. Jhang, and S. Lin, "Design of a wireless sensor network-based IoT platform for wide area and heterogeneous applications," *IEEE Sensors J.*, vol. 18, no. 12, pp. 5187–5197, Jun. 2018.

[6] S. Mayer, J. Hodges, D. Yu, M. Kritzler, and F. Michahelles, "An open semantic framework for the industrial Internet of Things," *IEEE Intell. Syst.*, vol. 32, no. 1, pp. 96–101, Jan./Feb. 2017.

[7] J. Wan, S. Tang, Q. Hua, D. Li, C. Liu, and J. Lloret, "Context-aware cloud robotics for material handling in cognitive industrial Internet of Things," *IEEE Internet Things J.*, vol. 5, no. 4, pp. 2272–2281, Aug. 2018.

[8] G. Han, L. Wan, L. Shu, and N. Feng, "Two novel DOA estimation approaches for real-time assistant calibration systems in future vehicle industrial," *IEEE Syst. J.*, vol. 11, no. 3, pp. 1361–1372, Sep. 2017.

[9] *Study on Channel Model for Frequencies From 0.5 to 100 GHz*, document 3GPP TR 38.901 V14.3.0 (2017-12), 3GPP-Technical Specification Group Radio Access Network, 2017.

[10] Y. Kondratenko, G. Kondratenko, and I. Sidenko, "Multi-criteria decision making for selecting a rational IoT platform," in *Proc. IEEE 9th Int. Conf. Dependable Syst., Services Technol. (DESSERT)*, May 2018, pp. 147–152.

[11] E. M. Silva, C. Agostinho, and R. Jardim-Goncalves, "A multi-criteria decision model for the selection of a more suitable Internet-of-Things device," in *Proc. Int. Conf. Eng., Technol. Innov. (ICE/ITMC)*, Jun. 2017, pp. 1268–1276.

[12] J. Haxhibeqiri, A. Karaagac, F. Van den Abeele, W. Joseph, I. Moerman, and J. Hoebeke, "LoRa indoor coverage and performance in an industrial environment: Case study," in *Proc. 22nd IEEE Int. Conf. Emerg. Technol. Factory Autom. (ETFA)*, Sep. 2017, pp. 1–8.

[13] T. Addabbo, A. Fort, M. Mugnaini, L. Parri, S. Parrino, A. Pozzebon, and V. Vignoli, "An IoT framework for the pervasive monitoring of chemical emissions in industrial plants," in *Proc. Workshop Metrol. Ind. 4.0 IoT*, Apr. 2018, pp. 269–273.

[14] *Short Range Devices; Low Throughput Networks (LTN); Protocols for Radio Interface A*, document ETSI TS 103 357 V1.1.1 (2018-06), 2018. Accessed: Mar. 2019.

[15] J. Petajajarvi, K. Mikhaylov, A. Roivainen, T. Hanninen, and M. Pettissalo, "On the coverage of LPWANs: Range evaluation and channel attenuation model for LoRa technology," in *Proc. 14th Int. Conf. ITS Telecommun. (ITST)*, Dec. 2015, pp. 55–59.

[16] M. Luvisotto, F. Tramarin, L. Vangelista, and S. Vitturi, "On the use of LoRaWAN for indoor industrial IoT applications," *Wireless Commun. Mobile Comput.*, vol. 2018, May 2018, Art. no. 3982646.

[17] M. Damsaz, D. Guo, J. Peil, W. Stark, N. Moayeri, and R. Candell, "Channel modeling and performance of Zigbee radios in an industrial environment," in *Proc. IEEE 13th Int. Workshop Factory Commun. Syst. (WFCS)*, May/Jun. 2017, pp. 1–10.

[18] R. M. Sandoval, A.-J. Garcia-Sanchez, and J. Garcia-Haro, "Improving RSSI-based path-loss models accuracy for critical infrastructures: A smart grid substation case-study," *IEEE Trans. Ind. Informat.*, vol. 14, no. 5, pp. 2230–2240, May 2018.

[19] W. Wang and E. S. Lohan, "Applicability of 3GPP indoor hotspot models to the industrial environments," in *Proc. 8th Int. Conf. Localization GNSS (ICL-GNSS)*, Jun. 2018, pp. 1–5.

[20] A. Alsayyari, I. Kostanic, C. Otero, M. Almeer, and K. Rukieh, "An empirical path loss model for wireless sensor network deployment in a sand terrain environment," in *Proc. IEEE World Forum Internet Things (WF-IoT)*, Mar. 2014, pp. 218–223.

[21] M. Soleimani, M. M. Bhuiyan, M. H. MacGregor, R. Kerslake, and P. Mousavi, "RF channel modelling and multi-hop routing for wireless sensor networks located on oil rigs," *IET Wireless Sensor Syst.*, vol. 6, no. 5, pp. 173–179, Oct. 2016.

[22] S. Shrestha, J. Talvitie, and E. S. Lohan, "Deconvolution-based indoor localization with WLAN signals and unknown access point locations," in *Proc. Int. Conf. Localization GNSS (ICL-GNSS)*, Jun. 2013, pp. 1–6.

[23] E. Tanghe, W. Joseph, L. Verloock, L. Martens, H. Capoen, K. Van Herwegen, and W. Vantomme, "The industrial indoor channel: Large-scale and temporal fading at 900, 2400, and 5200 MHz," *IEEE Trans. Wireless Commun.*, vol. 7, no. 7, pp. 2740–2751, Jul. 2008.

[24] M. Lauridsen, H. Nguyen, B. Vejlgaard, I. Z. Kovács, P. Mogensen, and M. Sorensen, "Coverage comparison of GPRS, NB-IoT, LoRa, and SigFox in a 7800 km^2 area," in *Proc. IEEE 85th Veh. Technol. Conf. (VTC Spring)*, Jun. 2017, pp. 1–5.

[25] B. Vejlgaard, M. Lauridsen, H. Nguyen, I. Z. Kovács, P. Mogensen, and M. Sorensen, "Interference impact on coverage and capacity for low power wide area IoT networks," in *Proc. Wireless Commun. Netw. Conf. (WCNC)*, Mar. 2017, pp. 1–6.

[26] *Semtech SX1276-7-8-9 Datasheet*. Accessed: Oct. 2018. [Online]. Available: https://www.semtech.com/uploads/documents/DS_SX1276-7-8-9_W_APP_V5.pdf

[27] (2018). *MIOTY^{TM} by BehrTech Starter Kit 1.0 with Microsoft Azure*. Accessed: Apr. 2019. [Online]. Available: https://cdn2.hubspot.net/hubfs/4739964/Data%20Sheets/BTI%20_%20Data%20Sheet%20Mioty%20Starter%20Kit%20v1.5%20(Print-Ready)%20April%2023.pdf?utm_campaign=Use%20Case%20-%20Downloads&utm_source=Website&utm_medium=Data%20Sheet

[28] J. Chen, K. Hu, Q. Wang, Y. Sun, Z. Shi, and S. He, "Narrowband Internet of Things: Implementations and applications," *IEEE Internet Things J.*, vol. 4, no. 6, pp. 2309–2314, Dec. 2017.

[29] A. Augustin, J. Yi, T. Clausen, and W. M. Townsley, "A study of LoRa: Long range & low power networks for the Internet of Things," *Sensors*, vol. 16, no. 9, p. 1466, 2016.

[30] M. Centenaro, L. Vangelista, A. Zanella, and M. Zorzi, "Long-range communications in unlicensed bands: The rising stars in the IoT and smart city scenarios," *IEEE Wireless Commun.*, vol. 23, no. 5, pp. 60–67, Oct. 2016.

[31] R. Quinnell, "Low power wide-area networking alternatives for the IoT," *EDN Netw.*, 2015. [Online]. Available: https://www.edn.com/design/systems-design/4440343/Low-power-wide-area-networking-alternatives-for-the-IoT
[32] D. M. Hernandez, G. Peralta, L. Manero, R. Gomez, J. Bilbao, and C. Zubia, "Energy and coverage study of LPWAN schemes for industry 4.0," in *Proc. IEEE Int. Workshop Electron., Control, Meas., Signals Appl. Mechatronics (ECMSM)*, May 2017, pp. 1–6.
[33] Y. Li, X. Cheng, Y. Cao, D. Wang, and L. Yang, "Smart choice for the smart grid: Narrowband Internet of Things (NB-IoT)," *IEEE Internet Things J.*, vol. 5, no. 3, pp. 1505–1515, Jun. 2018.
[34] R. E. Rider, "From cardinals to chaos: Reflections on the life and legacy of stanislaw Ulam," *Science*, vol. 246, no. 4926, pp. 134, 1989.
[35] D. P. Kroese, T. Taimre, and Z. I. Botev, *Handbook of Monte Carlo Methods*, vol. 706. Hoboken, NJ, USA: Wiley, 2013.
[36] O. Liberg, M. Sundberg, E. Wang, J. Bergman, and J. Sachs, *Cellular Internet of Things: Technologies, Standards, and Performance*. New York, NY, USA: Academic, 2017.
[37] *Spectrum Requirements for Short Range Device, Metropolitan Mesh Machine Networks (M3N) and Smart Metering (SM) Applications*, document ETSI TR 103 055 V1.1.1 (2011-09), 2011. Accessed: Mar. 2019.

WENBO WANG received the M.Sc. degree in electrical engineering from the Tampere University of Technology, Tampere, Finland, in 2016. He is currently pursuing the Ph.D. degree in wireless communication with Tampere University, Tampere. From 2016 to 2017, he was a Marie Curie Early Stage Researcher with the University of Twente, Enschede, The Netherlands. The research work focused on the efficient estimation of parameters in high-dimensional state space. His current research interests include the non-terrestrial networks, mmWave channel models, the industrial Internet-of-Things, and non-linear filtering algorithms. He has served as a Reviewer for the International Conference on Information Fusion, in 2018 and 2019, and as both a TPC member and a reviewer for the IEEE/CIC International Conference on Communications in China, in 2019.

STEFAN L. CAPITANEANU born in Bucharest, Romania, in 1976. He has received the Ph.D. degree in electrical engineering from the Institut National Polytechnique de Toulouse (INPT), France, in 2002. Since then, he has been with Schneider Electric. He is currently the Advanced Control Team Leader for the Industry Automation Department based near Paris, France. From milk drying to Eiffel hydraulic lift optimization, his work is used directly by big actors on European or world market as Sanofi, Lactalis, Agrial, Eiffel Tower Society, Areva, and Schlumberger. His main research interests include advanced process control, energy efficiency in industry by using process optimization, intelligent automation, and motor drives.

DANA MARINCA is currently an Associate Professor with the ALMOST Team (Algorithms and Stochastic Models), DAVID Laboratory (Data and Algorithms for Smart and Sustainable City), University of Versailles Saint-Quentin (UVSQ), University Paris Saclay. She has participated in four research projects funded by national and international institutions (EU FP7). Her research interests include recommendation systems, learning and prediction mechanism, and content delivery networks. She has coauthored more than 20 international peer-reviewed publications, has served as a TPC Member for several international conferences in networking, and has co-supervised so far five M.Sc. theses and two Ph.D. theses.

ELENA-SIMONA LOHAN received the M.Sc. degree in electrical engineering from the Polytechnics University of Bucharest, in 1997, the D.E.A. degree in econometrics from École Polytechnique, Paris, in 1998, and the Ph.D. degree in telecommunications from the Tampere University of Technology, in 2003. She is currently an Associate Professor with the Electrical Engineering Unit, Tampere University (formerly Tampere University of Technology) and a Visiting Professor with the Universitat Autonoma de Barcelona (UAB), Spain. She is leading a Research Group on Signal Processing for Wireless Positioning. She has co-edited the first book on galileo satellite system *Galileo Positioning Technology* (Springer), has co-edited a Springer book on multi-technology positioning, and has authored or coauthored more than 185 international peer-reviewed publications, six patents, and inventions. She has supervised more than 40 B.Sc./M.Sc. students and more than 13 Ph.D. students, ten of which completed their Ph.D. In the past four years, she has been a Principal Investigator in five national projects and four EU projects. She is also an Associate Editor for the *RIN Journal of Navigation* and for the *IET Journal on Radar, Sonar, and Navigation*.